Finite Element Analysis of Myocardial Diastolic Function Using Three-Dimensional Echocardiographic Reconstructions: Application of a New Method for Study of Acute Ischemia in Dogs

David D. McPherson, David J. Skorton, Srinivas Kodiyalam, Lawrence Petree, Michael P. Noel, Robert Kieso, Richard E. Kerber, Steve M. Collins, and Krishnan B. Chandran

The effect of acute myocardial ischemia on the myocardial elastic modulus has been a matter of controversy. To evaluate this question, diastolic elastic modulus was assessed by finite element analysis of left ventricular geometry using three-dimensional echocardiographic reconstructions and right and left ventricular pressure recordings. Elastic properties were estimated before and after coronary occlusion in 6 open-chest dogs. Elastic modulus values were derived by means of a computer program that determined the global elastic modulus that best predicted the diastolic changes in left ventricular geometry. In the finite element analysis after coronary occlusion, two analyses were performed: one utilizing the control elastic modulus for all segments of the left ventricle and one in which ischemic (dyskinetic) segments were assigned a higher elastic modulus. Results showed that the control elastic modulus was a poor predictor of diastolic left ventricular expansion after coronary occlusion. The finite element analysis in which the ischemic segments were assigned a higher elastic modulus better predicted ischemic diastolic wall motion patterns. Error values (difference between predicted and actual left ventricular segmental diastolic motion) were: control, 1.9 ± 0.3 mm (mean ± SD), ischemia, 2.9 ± 0.5 mm, and 2.2 ± 0.4 mm using the stiffer elastic modulus for ischemic segments. Error values were significantly higher ($p < 0.05$) under ischemic conditions when the control elastic modulus was uniformly applied compared with control and ischemia with dyskinetic segments assigned a higher elastic modulus. From these data, it is concluded that the myocardial diastolic elastic modulus is increased by ischemia and that this approach may allow clinical assessment of intrinsic muscle stiffness. (*Circulation Research* 1987;60:674–682)

The diastolic function of the left ventricle has become a topic of increasing interest to investigators and clinicians because of the mounting evidence of the importance of diastolic dysfunction in a variety of cardiac disorders.[1,2] There is new evidence indicating that abnormalities of myocardial mechanical properties during diastole not only may be independent of systolic mechanical abnormalities but also may precede systolic abnormalities.[3–5] Thus, a method that could demonstrate intrinsic myocardial diastolic abnormalities would be desirable. All of the models and methods developed to date[6–10] have shortcomings: some evaluated isolated muscle preparations,[6] some primarily evaluated pressure relations,[7] and others determined pressure-volume relations. Although pressure-volume relations are useful, they give an estimate of total chamber mechanical forces and do not allow evaluation of regional mechanical forces. Other shortcomings in studies to date include the assumption of spherical ventricular geometry,[6,8] the use of cast models to define ventricular geometry,[9] the use of two-dimensional (2D) cardiac imaging to determine complete three-dimensional (3D) ventricular geometry,[11] or the extrapolation of limited 2D cardiac images into a 3D network to define ventricular geometry.[10] Therefore, it is not surprising that in a recent review article, Glantz[12] stated that "no consensus has developed concerning how best to describe the diastolic left ventricle" and that "computing indices of diastolic stiffness has been counterproductive."

Two preliminary studies using finite element analysis[13,14] evaluated the properties of the elastic structure or modulus of the myocardium during normal and dis-

From the Cardiovascular Center and Departments of Internal Medicine, Electrical and Computer Engineering, Biomedical Engineering, and Radiology, University of Iowa, Iowa City, Iowa.

Supported in part by grant 2R01 HL27035 from the National Institutes of Health and by the F.E. Rippel Foundation. Dr. McPherson is the recipient of a Canadian Heart Foundation Fellowship and an Alberta Heritage Foundation for Medical Research Fellowship. Dr. Skorton is the recipient of Research Career Development Award K04 HL01290 from the National Heart, Lung, and Blood Institute.

Address for reprints: Krishnan B. Chandran, DSc, Department of Biomedical Engineering, University of Iowa, Iowa City, IA 52242.

Dr. McPherson's present address: Cardiology, Department of Internal Medicine, University of Calgary, 1403 29th NW, Calgary, Alberta, Canada T2N 2J9.

Received December 3, 1985; accepted January 13, 1987.

eased states. This technique described the regional properties of recovery of the myocardium from its end-systolic configuration to its end-diastolic configuration. However, it suffered primarily one major drawback: myocardial geometry was defined with multiple cineangiographic projections, a method that gives insufficient information on wall thickness. With the advent of 2D echocardiography, precise ventricular endocardial and epicardial border definitions could be obtained in many different planes. Our group[15] has recently shown in an animal model that 3D finite element reconstruction of the left ventricle can be obtained from cross-sectional echocardiographic images. This method takes multiple 2D images and, given the spatial coordinates of each image, then reconstructs the 3D shape. It does not require initial assumptions about ventricular geometry and should be useful in evaluation of regional mechanical changes.

An important clinical and physiologic question that remains in dispute is the effect of ischemia on myocardial elastic properties. Glantz and Parmley,[16] in a review of factors affecting the diastolic pressure-volume curve, cast doubt on the assertion that acute ischemia affects the ventricle's passive elasticity. However, more recent evidence[17,18] indicates that ischemia does indeed increase myocardial stiffness in a model of global ischemia. Therefore, finite element analysis and three-dimensional echocardiographic reconstructions were used to answer the following questions: Does acute ischemia alter the diastolic myocardial elastic modulus, and does the method of 3D reconstruction with finite element analysis accurately predict alterations in diastolic regional wall motion caused by ischemia? To study these questions, diastasis (that part of diastole after rapid filling and relaxation and before atrial systole) was evaluated. In diastasis, viscous and inertial effects are minimal, and passive elastic properties predominate.[3] The goal of this investigation was to combine previous advances in ultrasonic cardiac imaging with finite element analysis to form a new method that could evaluate ventricular diastasis.

Materials and Methods

Animal Preparations

Six mongrel dogs (weight, 18–25 kg) were anesthetized with intravenous sodium pentobarbital (30 mg/kg) and Innovar Vet (3 cc), intubated, and mechanically ventilated with room air. Femoral arterial and venous catheters were inserted for hemodynamic monitoring and vascular access. The ECG was continuously monitored. Calibrated transducer-tipped catheters (Mikrotip #MT-10, Millar Instruments Inc., Houston, Tex.) were inserted via the femoral artery and vein into the left and right ventricles for instantaneous high fidelity left and right ventricular pressure measurements. The thorax and pericardium were opened, and a pericardial cradle was constructed, stabilizing the heart within the thorax without altering ventricular hemodynamics. A snare was placed around the proximal circumflex coronary artery for later use in coronary occlusion.

Echocardiographic Recordings

The method of 3D echocardiographic recording has been previously reported.[15] Briefly, the 2.4 MHz phased-array transducer (Toshiba SSH-10A, Toshiba Inc., Japan) was attached to a mechanical position registration arm with 6 degrees of freedom that allowed determination of the relative positions and orientations of a set of 2D echocardiographic images with respect to a fixed external reference. An LSI 11/23 microcomputer (Digital Equipment Corporation, Maynard, Mass.) allowed the arm potentiometer readings to be digitized and stored in synchrony with echocardiographic recordings. The transducer was positioned over the right ventricle and was in light contact with the right ventricular epicardium. Thus, the right ventricle was used as a "standoff" so that left ventricular images could be obtained. Ten to twenty short-axis image recordings were obtained at mitral valve, chordal, papillary muscle, and apical levels for each experimental condition. The real-time images and the ECG were recorded onto ¾-inch videotape for subsequent playback and analysis of left ventricular geometry and wall motion. For each image orientation, simultaneous pressure measurements from the right and left ventricles were recorded on a strip chart recorder along with the ECG. The ECG was used as a time reference to correlate image (videotape) and pressure (strip chart) data. Also, the simultaneous potentiometer (orientation) data for each image were stored for later use in reconstruction. Variations in heart position due to respiration were minimized by acquiring data only at suspended end-expiration.

Experimental Protocol

Control 2D echocardiographic images were obtained as described above with simultaneous right and left ventricular pressure measurements and simultaneous transducer position information from the mechanical arm. Each animal was subsequently given 50 mg lidocaine i.v. and 5 mg/kg bretylium i.v. to prevent ventricular arrhythmias after coronary occlusion. After heart rate and blood pressure had returned to baseline levels (10–15 minutes), the circumflex coronary artery snare was tightened and the artery occluded. The animal was allowed to stabilize (5–10 minutes), and the ultrasound image collection protocol was repeated with simultaneous left and right ventricular pressure recordings and transducer position recordings from the mechanical registration arm.

After the postocclusion images were obtained, the animal was killed with intravenous KCl, and the heart was removed. In 4 dogs, a polyethylene cannula was inserted into the proximal left circumflex coronary artery just distal to the circumflex snare. Approximately 10 cc of carbon black particles and India ink were injected through the circumflex cannula to outline the circumflex perfusion field to the left ventricle. The heart was subsequently fixed in a 2.5% formalin-distilled water solution for a minimum of 72 hours. After fixation, the heart was sectioned into slices 1-cm thick, and the perfusion field areas outlined by the India ink

technique were marked and compared with the wall motion abnormalities (dyskinetic segments) identified on the real-time, 2D echocardiographic images. Light microscopy was then performed on hematoxylin and eosin stained segments from the ischemic and non-ischemic regions.

Three-Dimensional Echocardiographic Reconstructions

Three-dimensional reconstructions of left ventricular geometry from the 2D echocardiogrpahic images were obtained using an interactive computer program previously reported in detail.[15,19,20] A brief description of the procedure follows.

Before and after coronary occlusion, 3D reconstructions were performed at two points in the heart cycle: at early diastole (the nadir of left ventricular pressure) and at late diastole (just prior to the left ventricular pressure A wave). The ECG, which was recorded on both the strip chart (together with the right and left ventricular pressures) and on the echocardiographic videotape, was used as a time reference to correlate pressure and echo data and thus allow identification of the echo images corresponding to early and late diastole. From stop-frame images, the early and late diastolic endocardial and epicardial borders were traced from the video monitor onto transparent plastic sheets. Alignment marks on the border of the echocardiographic sector were also traced onto the plastic sheets. The traced borders were subsequently entered into a computer using a digitizing tablet. This method of echo image analysis has been used in previous studies,[21] and it has been found to be an accurate method of defining regional left ventricular wall motion.

The digitized epicardial and endocardial borders, together with the orientation data from the position registration arm, were used as input into an interactive reconstruction program. A standard coordinate system, fixed on the left ventricle, was defined with the origin located at the endocardial apex which was identified as described below (Figure 1). The z axis was defined as the line connecting the origin (endocardial apex) to the center of mass of the most basal (mitral valve) endocardial contour. The posterior junction of the right ventricular free wall and the ventricular septum (usually identified from a basal level image) was used as an anatomic landmark, and the direction of the line perpendicular to the z axis and passing through this landmark was determined. The x axis was defined as parallel to this line and passing through the origin. The y axis was defined as mutually perpendicular to the x and z axes. The digitized data for the endocardial and epicardial left ventricular borders were transformed to the standard coordinate system using Euler and Bryant angle transformations.[22]

The endocardial and epicardial apical points, which were not directly imaged, were "located" in the following manner. The endocardial apex was fixed on the z axis inferior to the most apical image at a distance that was the average endocardial radius (from the z axis) in the most apical image. The epicardial apex was fixed on the z axis inferior to the endocardial apex at a distance equal to the average wall thickness in the most apical image. With the use of the traced borders and the calculated apex points, a finite element mesh was formed. To generate finite elements of nearly equal volumes and to avoid skewed shapes, nodes (i.e., corners of the finite elements) were located on each of 7 parallel levels spaced at equal intervals between the apex and base of the reconstructed geometry. Eight nodes, spaced at equal angles, were located for each level for both the endocardium and epicardium. To avoid computational problems (i.e., singularity) that would arise if single endocardial and epicardial apical nodes were used to construct the apical elements, the apex points were each replaced with a small ring of 8 nodes. Thus, the reconstructed finite element mesh had 144 eight-noded solid isoparametric brick elements. Early and late diastolic left ventricular reconstructions for 1 dog are shown in Figure 2. It should be noted that the reconstructed geometry below the lowest apical level was an approximation to the actual geometry, as is illustrated by the conical apical cap in the reconstruction.

Finite Element Analysis

The hemodynamic and geometric data were evaluated by a finite element analysis technique. Discussions of finite element analysis in general and as applied to the evaluation of left ventricular mechanics are found elsewhere.[23–25] Details of our particular application of

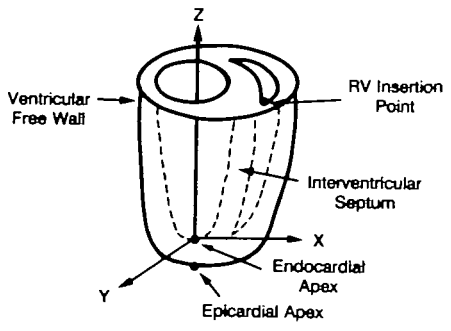

FIGURE 1. *Schematic diagram showing coordinate system fixed to left ventricular chamber.*

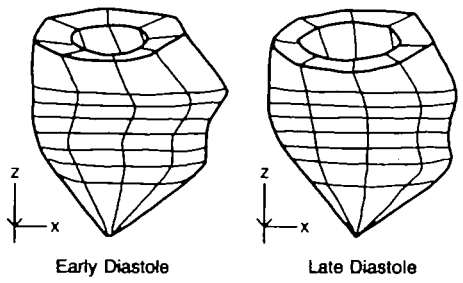

FIGURE 2. *Typical 3D ventricular reconstruction during early* (left) *and late* (right) *diastasis, plotted by the 3D graphics display program MOVIE-BYU (distributed by Brigham Young University).*

finite element analysis are found in the Appendix. The use of the finite element method in evaluation of left ventricular diastolic elastic properties in our study is reviewed briefly.

In general, the finite element method is begun by subdividing a complex 3D structure into smaller regions (finite elements) commonly taking the shape of bricks, where the corners of each element are referred to as nodes. In the usual application of finite element analysis, the geometry, material property (e.g., elastic modulus), and the forces acting on a complex 3D structure are known; the finite element technique is used to predict the displacement of the nodes (the alteration in size and shape of the structure) as the forces are applied. In our study, however, the forces acting on the left ventricular endocardium (change in diastolic pressure during diastasis) and the alteration in structure shape (change in left ventricular geometry from early to late diastiasis) were known from the recorded left ventricular pressure and 3D echocardiographic reconstructions. Hence, the finite element analysis was used to estimate left ventricular passive material properties. Our approach was to perform a finite element analysis on the early left ventricular diastolic geometry by initially assuming an elastic modulus for the myocardium. The finite element program was then used to predict the late diastolic geometry of the left ventricle, given the early diastolic geometry, the assumed elastic modulus, and the change in pressure during diastasis. The late diastolic geometry predicted by the finite element analysis was then compared with the actual late diastolic geometry determined from the echocardiographic reconstruction. The difference between the actual and computer-predicted geometry was termed the "error," and the assumed elastic modulus was modified and the finite element analysis repeated until the error was minimized. Our objective was to determine an optimal elastic modulus such that, given this elastic modulus, the early diastolic geometry, and the pressure change during diastasis, the computer-predicted diastolic expansion would closely match the actual diastolic expansion.

For our analysis, the force acting on the endocardial surface of the left ventricular chamber was specified as the measured left ventricular pressure difference from early to late diastasis. The right ventricular pressure difference from early to late diastasis was applied at the right endocardial surface of the ventricular septum. During the portion of diastole for which the analysis was performed (diastasis or slow filling), the myocardium was assumed to be a homogeneous, isotropic, linearly elastic material. To begin the finite element analysis, an assumed elastic modulus of 45,000 dyne/cm^2, an incompressible myocardium, and a Poisson's ratio of 0.49 were assumed.[26]

A schematic diagram of a representative finite element mesh along with the locations of the finite elements at various levels is shown in Figure 3. To estimate how well the computer-predicted late diastolic geometry matched the actual late diastolic geometry, an error function for each element was calculated (see

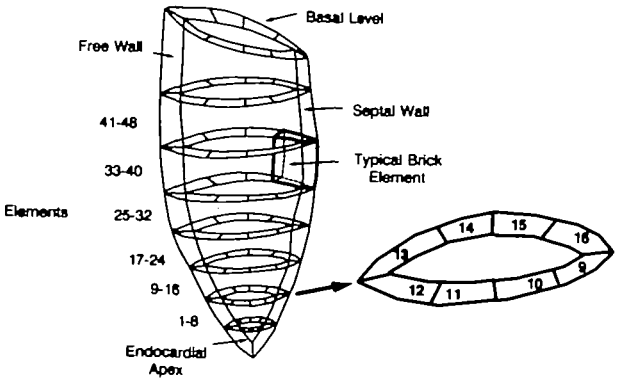

FIGURE 3. *Diastolic reconstruction in which finite elements have been identified for quantitative evaluation.*

Appendix) and plotted. For ease of interpretation and to approximate the coronary perfusion fields, the elements were plotted in groups with 2 septal elements, 2 posterior wall elements, 2 lateral wall elements, and 2 anterior wall elements identified for each of the levels from apex to base.

For evaluation of data obtained after the coronary artery occlusion, the finite element analysis was performed on the early diastolic geometry, using the optimal elastic modulus obtained for the corresponding control study. Should there be no changes in the passive myocardial elastic properties after acute ischemia, the error plot would be similar to that obtained in the control study. However, as described below, large errors were found in certain elements in the postocclusion study, indicating that the computer-predicted expansion poorly matched the actual expansion in these regions. The value of the elastic modulus was arbitrarily increased by 2, 3, 5, and 10 times for those elements exhibiting large errors (excluding the apical elements where the apical geometry was extrapolated and not measured). Elements to be assigned a higher elastic modulus were defined as those demonstrating errors greater than 1 SD above the mean for the postocclusion data. Increasing the elastic modulus (stiffness) by a factor of 10 reduced the combined error function toward control levels. Increasing the stiffness further did not improve the results appreciably. Hence, for the results presented in this work, the stiffness in the segments with large errors was increased by a factor of 10. Elements with increased errors were subsequently compared with the coronary perfusion fields (ischemic risk areas) obtained from the ink injection studies and with the region of wall motion abnormality identified on real-time echocardiograms.

Statistical Analysis

Analysis of variance was used to assess changes in the value of the combined error function (differences between predicted and actual nodal displacements) between the baseline state, ischemic state, and ischemic state with the dyskinetic segments assigned a higher elastic modulus. All group data are expressed as mean ± SD.

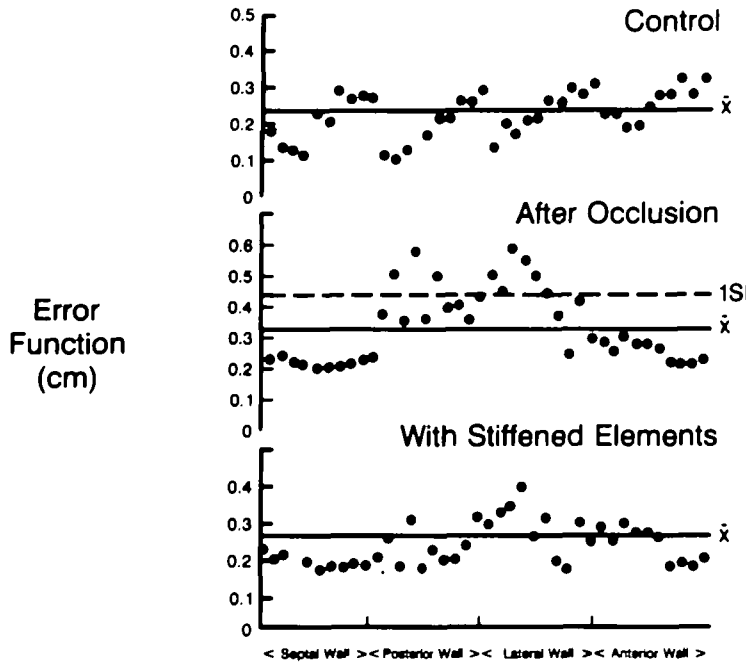

FIGURE 4. *Plot of error function for each finite element in a single animal study:* top, *control;* middle, *postocclusion;* bottom, *postocclusion with stiffened ischemic elements. Elements are plotted in septal, posterior wall, lateral wall, and anterior wall groups from level above apex to base to approximate coronary perfusion fields.*

Results

A plot of the error function calculated for each finite element for a single animal study is shown in Figure 4. The mean error for all the elements is also shown in the figure. The error plot for the control study (Figure 4, top) shows a mean error of 0.23 cm. The apical level, where the geometry has been approximated, is not included. In the control study, the error for any single element did not exceed 0.32 cm. For this dog, the optimized control elastic modulus was computed to be 20,000 dynes/cm^2. The optimal elastic moduli computed from the control experiments on the 6 open-chest dogs are presented in Table 1.

The error plot for the postocclusion analysis for the same dog (Figure 4, middle) shows a mean error of 0.32 cm and errors as large as 0.60 cm in certain elements. The elements with errors in the upper 33% of the variation (more than 1 SD above the mean error), lying primarily within the posterior and lateral wall, were stiffened by 10 times, as described above. The error plot with the stiffened elements (Figure 4, bottom) shows that the mean error was reduced to 0.27 cm with the largest error of less than 0.50 cm. The elements with errors in the upper 33% are those above the 1-SD line in the error plot shown in the middle panel of Figure 4.

When the mean value of the error for all elements for each dog was separately evaluated, it was observed that for all 6 dogs, the mean error for the postocclusion study increased compared with the control study. Also, when the elastic modulus values in elements with large errors were increased by 10 times, the mean error diminished and approached the value of the control study.

Figure 5 illustrates the differences (errors) between the predicted and actual left ventricular segmental diastolic nodal displacements (cavity expansion) for the control animals, postocclusion animals, and postocclusion animals in which the ischemic segments were assigned a stiffer elastic modulus. The control and stiffened postocclusion data fit the actual wall motion

Table 1. Pressure Differences (Late Diastole-Early Diastole) and Optimized Elastic Modulus (E)

Dog No.	Left ventricular pressure (mm Hg)	Right ventricular pressure (mm Hg)	Optimized E (dyne/cm^2)
1446	3.00	3.00	30,000
1451	5.50	3.00	20,000
1452	6.25	4.00	37,000
1458	4.25	2.75	43,000
1462	5.00	3.50	36,000
1463	3.75	1.25	15,500
Mean	4.63	2.92	30,265
SD	1.09	0.85	9.705

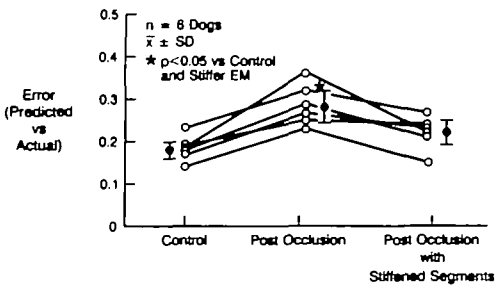

FIGURE 5. *Errors between the predicted and actual left ventricular diastolic expansion for control data, postocclusion data analyzed using control elastic modulus, and postocclusion data analyzed using stiffer elastic moduli for ischemic segments.*

better than the postocclusion data in which all elements were assigned the same (control) elastic modulus. Statistical analysis revealed significant differences ($p < 0.05$) between the mean error under control conditions (1.9 ± 0.3 mm) compared with the mean error with ischemia (2.9 ± 0.5 mm) and between the mean error with ischemia compared with the mean error with ischemia and stiffer ischemic segments (2.2 ± 0.4 mm).

In the animals in which India ink/carbon black staining was performed, the perfusion field of the left circumflex coronary artery, identified by the stain, lay within the 2D echocardiographic wall motion abnormality field, identified after the creation of acute ischemia. Histologic specimens revealed evidence of early ischemia (cell swelling and contraction banding) in the ischemic areas only but did not show major histologic abnormalities indicative of more severe or permanent damage.

Discussion

Finite element analysis of 3D echocardiographic reconstructions was used to demonstrate that acute ischemia increases regional stiffness of the myocardium. The present analysis has demonstrated that the difference between the computer-predicted diastolic expansion and the actual expansion increased in the region of acute ischemia. In these regions, the use of an optimal elastic modulus obtained from the control study in the postocclusion finite element analysis overpredicts the diastolic deformation. By increasing the elastic modulus in these segments, the error between the predicted and the actual deformation decreases, thus indicating a stiffening of the passive elastic modulus in the region affected by the acute ischemia.

Comparison With Prior Observations

Using a similar technique on images obtained from biplane cineangiography on humans, Ray et al[13,14] have shown that the myocardial passive elastic modulus increases (indicating a stiffening) in regions of suspected infarction. These data support the work by Visner et al,[17] Sasayama et al,[18] and Hess et al[27] that ischemia increases myocardial diastolic stiffness. Visner[17] evaluated a model of global ventricular ischemia in an attempt to separate the results of direct ischemia from the interactions between ischemic and surrounding nonischemic myocardium. This was one of the first papers to show that alterations in regional diastolic mechanics are the direct result of ischemia. In a model of global ischemia, Sasayama et al[18] used a patient model of pacing-induced ischemia to evaluate diastolic segment length alterations. They found that ischemia-induced alterations in diastolic pressure were associated with smaller changes in diastolic expansion of the ischemic vs. the nonischemic segments. Although the results of that study are similar to ours, their patient model, of necessity, relied on analysis of a single 2D ventricular angiogram to differentiate ischemic from nonischemic myocardium.

Paulus et al[28] assessed regional myocardial function in dogs following pacing tachycardia with coronary stenosis and coronary occlusion. Measuring regional segmental lengths and wall thickness, their analysis showed that the regional properties of the myocardium were different with coronary occlusion and stenosis. Earlier, Bourdillon et al[29] showed that the regional myocardial stiffness of the left ventricle in humans increased during pacing-induced ischemia. The present study, using a more sophisticated approach based on finite element analysis of the 3D geometry of the LV chamber, confirmed their results on the regional changes in the myocardial material properties.

What are the mechanisms responsible for the observed ischemia-induced alteration in intrinsic myocardial material properties? Myocardial relaxation is altered by ischemia, but our data were essentially obtained during diastasis when active myocardial relaxation is presumably largely complete. Alterations in coronary vascular turgor, systolic stretch, and accumulation of hydrogen ions have been implicated by Momomura et al[30] in their study of mechanical and biochemical events related to ischemia-induced diastolic dysfunction. Although our study was not designed to delineate the mechanisms responsible for ischemia-induced alterations in diastolic myocardial material properties, one important implication of our findings is that in coronary occlusion-induced ischemia, intrinsic muscle stiffness is altered. This finding stands in contrast to the apparent lack of alteration in left ventricular pressure-segment length relations in the study by Momomura and coworkers.[30] Since other studies have suggested that regional myocardial stiffness is increased in coronary occlusion-induced ischemia in dogs,[31] our data, derived from a different analytic technique, extend the previous observations and add to the base of knowledge of the complex relations between myocardial perfusion and diastolic function.

Advantages of Present Method

The method of estimating myocardial stiffness based on 3D reconstruction enables more precise evaluation of cardiac geometry and motion than previous methods, which used limited 2D cardiac motion patterns. The method of finite element analysis, initially proposed by Ray et al[13,14] and modified here to fit the 3D reconstruction, accurately evaluates and predicts wall motion relations and alterations in mechanical properties throughout the cardiac chamber. Finite element analysis is the only method available at present that can evaluate regional variability in elasticity from a global 3D model. All other methods presume similar changes in wall motion patterns for the total geometric shape being evaluated. The inability to evaluate regional ventricular geometry and regional mechanical changes may in part explain previous contradictory data indicating that ischemia does or does not alter myocardial diastolic stiffness.[16] Those previous studies were unable to evaluate regional left ventricular function over the entire left ventricle. Templeton et al[32] used a global ventricular model to evaluate elastic diastolic changes with ischemia. Tyberg et al[33] and Palacios et al[34] used multiple one-dimensional measure-

ments to evaluate regional ventricular diastolic function. The method used in the present study circumvents these problems by evaluating regional function over the entire ventricle.

Limitations

In the present study, the myocardium was assumed to exhibit linear elastic properties. It is well known that the myocardium has nonlinear stress-strain behavior. Even during the portion of diastole where the analysis is performed, a stepwise linear analysis might be used to account for the nonlinearity. However, such an analysis would require reconstruction of the left ventricular chamber at several points during the diastolic period. The images are obtained from multiple cycles at 33-millisecond intervals, and problems also exist in the detection of endocardial and epicardial borders. In the postocclusion studies, only a limited number of images were available during diastasis due to the rapid heart rates. Hence, it was felt that the errors introduced in the reconstruction procedure did not justify a stepwise linear analysis. Moreover, the elastic modulus of the myocardium was used as a parameter that shows a change after acutely induced ischemia. Thus, it was assumed that the myocardium is made of linear elastic material during the part of diastole in which the analysis was performed. Image acquisition systems that acquire images rapidly (such as rapid acquisition computed tomography) may allow for multiple images in diastasis to evaluate the nonlinear myocardial elastic properties. The present method of 3D reconstruction requires many cardiac cycles for data acquisition and cannot construct a 3D image from a single cardiac cycle. An assumption that geometry does not change over the multiple cycles of data acquisition must be made, and although probably true in the control setting, this may not be true after interventions have been made. Echocardiographic image quality in the closed-chest animal or patient population is inconsistent and could not routinely give data as reproducible and accurate as were obtained from our open-chest preparation. Newer techniques are presently being developed, such as rapid acquisition computerized tomography, that may allow more accurate 3D cardiac reconstruction in the patient population.[35] Since each ventricular level was divided into only 8 finite elements, some variable wall motion may have occurred within each segment. A finite element analysis procedure that divides each level into a larger number of segments should reduce variability of wall motion within each segment. Finally, an increase of elastic modulus changing from control to intervention has been described, not the absolute elastic modulus, which is beyond the scope of this model.

Implications

In conclusion, a technique and model to evaluate ventricular diastolic mechanical properties have been described, and it has been shown that acute ischemia increases the elastic modulus in the involved segments. This integrated approach to regional cardiac mechanics has far-reaching implications. Now, not only can pathologic changes be evaluated on a regional basis, but the effects of interventions on cardiac mechanics can be more accurately evaluated on the involved and distant segments. Hopefully, this method will permit more consistent and representative data to be obtained from future experiments evaluating ventricular mechanics.

Appendix

Finite Element Analysis

The finite element method is an approximate numerical solution procedure that uses the digital computer to solve complex structural problems where closed-form solutions of the governing equations are mathematically intractable.[23,24] This procedure has found wide application in problems involving the mechanics of complex biologic structures such as the left ventricle.[25] In the finite element method, a complex 3D structure is subdivided into smaller regions, called finite elements, which commonly take the shape of bricks. The corners of each brick element are referred to as nodes. Using available laws of mechanics, equations governing the elements are derived in terms of the nodal displacements. For a static (time-independent) analysis, the assembled equations are of the form:

$$[K]\{\delta\} = \{F\} \quad (1)$$

In this equation, [K] is the stiffness matrix which is based on the nodal coordinates (geometry) and the material property of the structure, $\{\delta\}$ is a vector of nodal displacements, and {F} is the vector of forces to which the structure is subjected. The boundary conditions are usually specified in the form of known displacements of the nodes lying on the boundary, i.e., where the structure is attached to another supporting structure.

In the usual finite element analysis described above, the geometry, material property, and the forces on a structure are known, and the nodal displacements are directly solved for using equation 1. However, in the present study, the geometry of the "deformed" structure (late diastolic reconstructed mesh) was known, as was the load on the structure (pressure change during diastole). Hence, this analysis was treated as an inverse problem where the passive elastic modulus of the myocardium was an unknown. The finite element analysis was performed on the early diastolic geometry with an assumed elastic modulus for the myocardium. The finite element program was used to predict the late diastolic geometry of the left ventricle, given the early diastolic geometry, an assumed elastic modulus, and the diastolic pressure change. The computer-predicted late diastolic geometry was compared with the actual late diastolic geometry from the reconstruction. The difference between the actual and the computer-predicted geometry was termed the "error," and the assumed elastic modulus was modified using an optimization technique described below, until the "error" was minimized. A general-purpose finite element analysis program (ANSYS, Swanson Analysis, Inc., Houston,

Penn.) was applied in the interactive mode to the finite element mesh for the early diastolic geometry. The nodes on the most basal (mitral) level were fixed and served as the boundary condition. It was assumed that the LV at early diastole is at the nadir of the pressure wave, i.e., that the ventricular relaxation is complete at this point. The load on the endocardial surface of the left ventricular chamber was specified as the measured left ventricular pressure difference between early and late diastole. The RV pressure difference between early and late diastole was applied at the right endocardial surface of the ventricular septum. The only other required input for the finite element analysis was the passive material property of the myocardium. This study was designed to compute an index that is sensitive to a change in myocardial material property (as opposed to the absolute elastic modulus) when a region of the myocardium becomes ischemic. During the portion of diastole for which the analysis was performed, the myocardium was assumed to be a homogeneous, isotropic, Hookean elastic material. An assumed elastic modulus (E_I = 45,000 dyne/cm^2) was specified to start the finite element analysis. The myocardium was assumed to be incompressible, and a Poisson's ratio of 0.49 was also assumed.[26]

In this linear elastic problem, the displacements of the nodes will be inversely proportional to the magnitude of the elastic modulus. In other words, the larger the elastic modulus, the stiffer the material, and the displacements will be proportionately reduced for the same load. The objective was to determine an "optimal" elastic modulus, E_{opt}, such that given 1) the elastic modulus, 2) the early diastolic geometry, and 3) the pressure change during diastole, the computer-predicted diastolic expansion would closely match the actual late diastolic geometry.

In the usual optimization scheme, the assumed E_I would be modified using an optimization algorithm and the finite element analysis repeated until an index of performance was minimized. However, the present linear analysis took advantage of the fact that the nodal displacements were linearly but inversely proportional to the elastic modulus. Hence, E_{opt} was determined by computing a scale factor, α, such that

$$E_{opt} = \frac{E_I}{\alpha} \qquad (2)$$

The details for computing the scale factor, α, are as follows: Let x_{iE} be the x coordinate of the node i in early diastole and x_{iL} be the corresponding x coordinate in late diastole, as schematically shown in Figure 6. Let dx_i be the displacement in the x direction of node i, as determined by the finite element analysis program. Let α be the scale factor by which the displacement dx_i is modified so that the difference between the x coordinate of the predicted node position ($x_{iE} + \alpha dx_i$) and that of the actual node position (x_{iL}) is reduced. Considering the x coordinates of all the nodes in the finite element mesh, and error Q_x was defined as

$$Q_x(\alpha) = \frac{1}{N}\sum_{i=1}^{N}(x_{iE} + \alpha dx_i - x_{iL})^2 \qquad (3)$$

where N is the number of nodes.

Similarly, errors in the y and z direction were calculated by the relations

$$Q_y(\alpha) = \frac{1}{N}\sum_{i=1}^{N}(y_{iE} + \alpha dy_i - y_{iL})^2 \qquad (4)$$

$$Q_z(\alpha) = \frac{1}{N}\sum_{i=1}^{N}(z_{iE} + \alpha dz_i - z_{iL})^2 \qquad (5)$$

A combined error, Q, an index of the difference between predicted and actual diastolic nodal displacements, was defined as

$$Q(\alpha) = w_xQ_x + w_yQ_y + w_zQ_z \qquad (6)$$

where w_x, w_y, and w_z were weighting factors selected such that $w_x + w_y + w_z = 1$. The assigned values for the weighting factors were $w_x = w_y = 0.45$ and $w_z = 0.1$. The "z axis" resolution of the imaging technique was poorer than the x and y axis resolution, and thus, weighting was heavier in the x and y directions.

The optimal value of the scale factor, α, was obtained when the value of the error function in equation 6 was minimized. The optimum scale factor was determined by differentiating equation 6 with respect to α and setting the derivative to zero. The resulting optimal value for α was used to compute the elastic modulus, E_{opt}, using equation 2. To estimate how well the computer-predicted late diastolic geometries matched the actual late diastolic geometries, an error function (defined as the sum of the square root of the errors in each coordinate direction multiplied by the weighting factors) was calculated and plotted. The error function is expressed in centimeters.

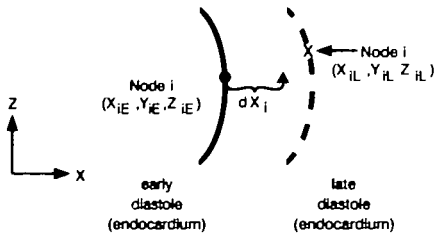

FIGURE 6. *Schematic diagram of actual and computer-predicted positions of node i; dx_i, predicted nodal displacement during diastole.*

Acknowledgment

We would like to acknowledge the expert secretarial assistance of Marlene Blakley and Rita Yeggy in preparing this manuscript.

References

1. Mann T, Goldberg S, Mudge GH, Grossman W: Factors contributing to altered left ventricular diastolic properties during angina pectoris. *Circulation* 1979;59:14–20
2. Grossman W: Why is left ventricular diastolic pressure in-

creased during angina pectoris? *J Am Coll Cardiol* 1985;5: 607–608
3. Grossman W, McLaurin LP: Diastolic properties of the left ventricle. *Ann Intern Med* 1976;84:316–326
4. Hirota Y: A clinical study of left ventricular relaxation. *Circulation* 1980;62:756–763
5. Dougherty AH, Naccarelli GV, Gray EL, Hicks CH, Goldstein RA: Congestive heart failure with normal systolic function. *Am J Cardiol* 1984;54:778–782
6. Mirsky I, Parmley WW: Assessment of passive elastic stiffness for isolated heart muscle and the intact heart. *Circ Res* 1973;33:233–243
7. Schaff HV, Gott VL, Goldman RA, Frederiksen JW, Flaherty JT: Mechanism of elevated left ventricular end-diastolic pressure after ischemic arrest and reperfusion. *Am J Physiol* 1981;240:H300–H307
8. Glantz SA, Kernoff RS: Muscle stiffness determined from canine left ventricular pressure-volume curves. *Circ Res* 1975; 37:787–794
9. Janicki JS, Weber KT, Gochman RB, Shroff S, Geheb FJ: Three-dimensional myocardial and ventricular shape: A surface representation. *Am J Physiol* 1981;241:H1-H11
10. Vinson CA, Gibson DG, Yettram AL: Analysis of left ventricular behaviour in diastole by means of finite element method. *Br Heart J* 1979;41:60–67
11. Mirsky I, Cohn PF, Levine JA, Gorlin R, Herman MV, Kreulen TH, Sonnenblick EH: Assessment of left ventricular stiffness in primary myocardial disease and coronary artery disease. *Circulation* 1974;50:128–136
12. Glantz SA: Computing indices of diastolic stiffness has been counterproductive. *Fed Proc* 1980;39:162–168
13. Ray G, Ghista DN, Sandler H: In vivo constitutive properties of the passive left ventricular myocardium. *ASME Biomechanics Symposium*. New York, American Society of Mechanical Engineers, 1979, pp 129–132
14. Ray G, Ghista DN, Sandler H: Left ventricular biomechanical analyses for the development of indices characterizing normal-diseased myocardium and left ventricular pumping efficiency, in Ghista DN, Van Vollellhoven E, Yang WJ, Reul H (eds): *Advances in Cardiovascular Physics*, Vol 4: *Foundations of Noninvasive Cardiovascular Diagnostic Processes*. Basel, Switzerland, S. Karger, 1979, pp 161–178
15. Nikravesh PE, Skorton DJ, Chandran KB, Attarwala YM, Pandian N, Kerber RE: Computerized three-dimensional finite element reconstruction of the left ventricle from cross-sectional echocardiograms. *Ultrason Imaging* 1984;6:48–59
16. Glantz SA, Parmley WW: Factors which affect the diastolic pressure-volume curve. *Circ Res* 1978;42:171–180
17. Visner MS, Arentzen CE, Parrish DG, Larson EV, O'Connor MJ, Crumbley AJ III, Bache RJ, Anderson RW: Effects of global ischemia on the diastolic properties of the left ventricle in the conscious dog. *Circulation* 1985;71:610–619
18. Sasayama S, Nonogi H, Miyazaki S, Sakurai T, Kawai C, Eiho S, Kuwahara M: Changes in diastolic properties of the regional myocardium during pacing-induced ischemia in human subjects. *J Am Coll Cardiol* 1985;5:599–606
19. Chandran KB, Olshansky B, Attarwala Y, Skorton DJ: Finite element analysis of 3-D echocardiographic data in the evaluation of diastolic left ventricular function. *Automedica* 1984; 5:151–169
20. Skorton DJ, Chandran KB, Collins SM, Petree LP, McPherson DD, Olshansky B, Noel MP, Kerber RE: Three-dimensional ultrasonic cardiac reconstruction: General aspects and application to finite element analysis of the left ventricle, in Sideman S, Beyar R (eds): *Simulation and Imaging of the Cardiac Systems*. 1985, Boston, Martinus Nijhoff Publishers, pp 174–189
21. Pandian NG, Skorton DJ, Doty DB, Kerber RE: Immediate diagnosis of acute myocardial contusion by two-dimensional echocardiography: Studies in a canine model of blunt chest trauma. *J Am Coll Cardiol* 1983;2:488–496
22. Wittenberg J: *Dynamics of Systems of Rigid Bodies*. Stuttgart, BG Teubner, 1977
23. Cook RD: *Concepts and Applications of Finite Element Analysis*, ed. 2. New York, John Wiley and Sons, 1981
24. Desai CS: *Elementary Finite Element Method*. New Jersey, Prentice-Hall Inc, 1970
25. Yin FCP: Ventricular wall stress. *Circ Res* 1977;49:829–842
26. Caro CG, Pedley TJ, Schroter RC, Seed WA: *The Mechanics of Circulation*. Oxford, England, Oxford University Press, 1978, p 89
27. Hess OM, Koch R, Bamert C, Krayenbuehl HP: Regional wall stiffness during acute myocardial ischemia in the canine left ventricle. *Eur Heart J* 1980;1:435–443
28. Paulus WJ, Grossman W, Serizawa T, Bourdillon PD, Pasipoularides A, Mirsky I: Different effects of two types of ischemia on myocardial systolic and diastolic function. *Am J Physiol* 1985;248:H719–H728
29. Bourdillon PD, Lorell BH, Mirsky I, Paulus WJ, Wynne J, Grossman W: Increased regional myocardial stiffness of the left ventricle during pacing-induced angina in man. *Circulation* 1983;67:316–323
30. Monomura S, Ingwall JS, Parker JA, Sahagian P, Ferguson JJ, Grossman W: The relationships of high energy phosphates, tissue pH, and regional blood flow to diastolic distensibility in the ischemic dog myocardium. *Circ Res* 1985;57:822–835
31. Hess OM, Osakada G, Lavelle JF, Gallagher KP, Kemper WS, Ross J Jr: Diastolic myocardial wall stiffness and ventricular relaxation during partial and complete coronary occlusions in the conscious dog. *Circ Res* 1983;52:387–400
32. Templeton GH, Wildenthal K, Willerson JT, Mitchell JH: Influence of acute myocardial depression on left ventricular stiffness and its elastic and viscous components. *J Clin Invest* 1975;56:278–285
33. Tyberg JV, Forrester JS, Wyatt HL, Goldner SJ, Parmley WW, Swan HJC: An analysis of segmental ischemic dysfunction utilizing the pressure-length loop. *Circulation* 1974; 49:748–754
34. Palacios I, Johnson RA, Newell JB, Powell WJ Jr: Left ventricular end-diastolic pressure volume relationships with experimental acute global ischemia. *Circulation* 1976;53: 428–436
35. Collins SM, Yashodar P, Rumberger JA, Feiring AJ, Noel MP, Chandran KB, Fleagle SR, Marcus ML, Skorton DJ: Three-dimensional reconstruction of the contracting canine heart using cine computed tomography, in *1985 Computers in Cardiology*. Long Beach, Calif, IEEE Computer Society, 1985, pp 67–72

KEY WORDS • left ventricle • myocardium • diastolic properties • finite element analysis • 3D reconstruction • echocardiography